

Figure 2. Schematic diagram of mutation sites on (A) cardiac ryanodine receptor (*RYR2*), (B) calyculin 2 (*CASQ2*), and (C) inward rectifier potassium channel 2 (*KCNJ2*). Red, mutation sites identified in the present study; purple, those previously reported. FKBP, 12.6 (calyculin) binding domain; TMD, transmembrane domain.

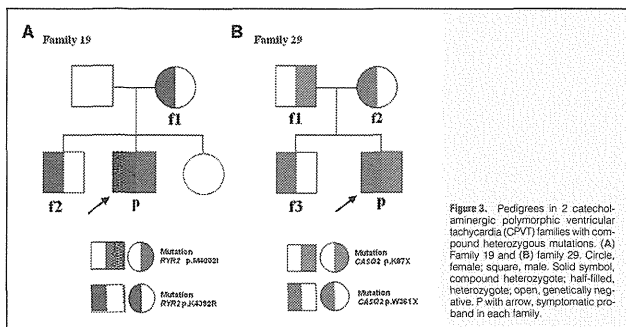


Figure 3. Pedigrees in 2 catecholaminergic polymorphic ventricular tachycardia (CPVT) families with compound heterozygous mutations. (A) Family 19 and (B) family 29. Circle, female; square, male. Solid symbol, compound heterozygote; half-filled, heterozygote; open, genetically negative. P with arrow, symptomatic proband in each family.

bands (incidence: 56.0%); exon3 deletion, p.R169Q, p.R407S, p.R420Q, p.N151S, p.M2192L, p.S2246L, p.A2287V, p.G2400T, p.R2474G, p.G2628E, p.D3638A, p.Q3861H, p.P3876E, p.G3946S, p.M4002I, p.K4392R, p.L4105F, p.S4124R, p.N4178S, p.L4587V, p.Y4725C, p.K4750Q, p.V4771I, p.L4865V, and p.L4919S (Table 1; Figure 2A). All patients were heterozygous and 18 of the mutations were novel. Table 1 lists genetic and clinical data of all the individuals who carried genetic mutations, including the family members. We examined 46 relatives of 28 probands with *RYR2* muta-

Circulation Journal Vol.77, July 2013

	Total (n=47)	<i>RYR2</i> -positive CPVT (n=27)	<i>RYR2</i> -negative CPVT (n=20)	P-value
β-blockers	43 (91.5)	27 (100.0)	16 (80.0)	0.027
β-blockers+only	27 (57.4)	16 (59.3)	11 (55.0)	NS
Flecainide	8 (17.0)	6 (22.2)	2 (10.0)	NS
Verapamil	9 (19.1)	6 (22.2)	3 (15.0)	NS
Verapamil+only	1 (2.1)	0 (0)	1 (5.0)	NS
Amiodarone	1 (2.1)	0 (0)	1 (5.0)	NS
Combination				
β-blockers+verapamil	4 (8.5)	3 (11.1)	1 (5.0)	NS
β-blockers+ICD	3 (6.4)	1 (3.7)	2 (10.0)	NS
β-blockers+flecainide	2 (4.3)	2 (7.4)	0 (0)	NS
β-blockers+verapamil+ICD	1 (2.1)	1 (3.7)	0 (0)	NS
β-blockers+flecainide+ICD	3 (6.4)	2 (7.4)	1 (5.0)	NS
β-blockers+verapamil+flecainide	2 (4.3)	1 (3.7)	1 (5.0)	NS
β-blockers+verapamil+flecainide+ICD	1 (2.1)	1 (3.7)	0 (0)	NS
ICD	8 (17.0)	5 (18.5)	3 (15.0)	NS
No medication	2 (4.3)	0 (0)	2 (10.0)	NS

Data given as n (%). CPVT, catecholaminergic polymorphic ventricular tachycardia. Other abbreviations as in Table 1.

(Figure 1) was documented in 17 cases (36.2%), pVT in 31 (66.0%) and VF in 16 (34.0%) on ECG in the absence of medication. Atrial fibrillation was noted in 1 proband (2.1%), atrial flutter in 1 (2.1%), atrial tachycardia in 2 (4.3%) and supraventricular tachycardia in 2 (4.3%). All types of arrhythmias were paroxysmal and induced by exercise.

#### Clinical Characteristics of *RYR2* Mutation-Positive vs. -Negative CPVT

In order to characterize the clinical features of CPVT patients, we divided them into 2 groups (Table 2): *RYR2* mutation positive (n=27) and negative (n=20). Among 27 *RYR2* mutation carriers, there were only 11 male carriers (40.7%). The number of probands whose family members were clinically diagnosed as having CPVT was significantly larger in the *RYR2* mutation-positive group (P=0.018). Exercise-induced bVT (P=0.043) and sinus bradycardia (P=0.021) were significantly more frequent in the *RYR2* mutation-positive patients. In contrast, atrial arrhythmias were detected at a similar frequency in both groups (P=0.261).

#### Exercise Stress Test

Thirty-one probands of 4-7 underwent exercise stress tests. The remaining 16 subjects were not examined because of cerebral palsy, hypoxic brain damage at the first attack or diagnosis on other examinations such as Holter monitoring ECG. Thirty probands of 31 developed various arrhythmias during exercise stress test and were judged as positive probands; 19 of them were found to carry *RYR2* mutations (Table 1). The prevalence of positive stress test was not statistically different between the mutation-positive and -negative groups (Table 2).

#### Treatment

There were 47 symptomatic probands, and 45 of them received medical treatment (Table 3). Two probands who were not genotyped had no medication. β-blockers were prescribed in 43 patients (91.5%); 27 of them (57.4%) were treated with β-blockers alone, and the other 16 probands took them in combination with other medication and/or implantable cardiover-

ter-defibrillator (ICD) implantation. Beta-blocker treatment was significantly more prevalent (P=0.027) in the *RYR2* mutation-positive probands (Table 3), and there was a tendency for more of them to receive combination therapy with β-blockers and verapamil or flecainide or ICD. ICD was used in 5 *RYR2*-positive and 3 mutation-negative probands, and all received β-blockers simultaneously, which appeared to partially protect against subsequent ICD shock delivery (mean follow-up period, 63 months). Two of them (1-p, 2-p; Table 1) received appropriate ICD therapy. Flecainide was prescribed in 6 *RYR2* mutation-positive patients, which was frequently more prescribed in the *RYR2* mutation-positive than negative group and in all cases it suppressed ventricular tachycardia or ventricular extrasystoles on exercise test.

Among *RYR2*-positive probands first treated with β-blockers alone, 5 (19%) were refractory to β-blockers with recurrent syncope (mean follow-up, 48 months), and additional flecainide therapy was then introduced, which was successful in all cases. The detailed clinical outcome is reported elsewhere.<sup>24</sup>

#### Discussion

In the present study, we first screened for gene mutations in a considerable number of Japanese CPVT patients and summarized the clinical data. The major findings are as follows: (1) in 50 clinically diagnosed CPVT probands, we identified 26 different *RYR2* mutations in 28 probands (CPVT1; incidence, 56.0%); (2) we identified probands with compound heterozygous *RYR2* mutations, compound heterozygous *CASQ2* mutations and heterozygous missense *KCNJ2* mutation in 1 family each, respectively; (3) the number of probands whose family members were clinically diagnosed as having CPVT was significantly larger in the *RYR2* mutation-positive group, and exercise-induced bVT was significantly more prevalent in the *RYR2* mutation-positive patients; and (4) β-blocker treatment was significantly more prevalent (P=0.027) in *RYR2* mutation-positive probands, and there was a tendency for more of them to receive combination therapy with β-blockers and verapamil or flecainide or ICD.

	Total (n=47)	<i>RYR2</i> -positive CPVT (n=27)	<i>RYR2</i> -negative CPVT (n=20)	P-value
Male	19 (40.4)	11 (40.7)	8 (40.0)	NS
Mean age at onset (years)	10.2±7.3	8.6±4.7	12.6±9.9	NS
Family history of sudden death	17 (14.9)	8 (22.2)	9 (50.0)	0.018
Clinically diagnosed CPVT family members	10 (21.3)	9 (33.3)	1 (5.0)	0.018
Mean HR (beats/min)	62±14	59±14	67±13	NS
Mean QTc (ms)	424±28	426±21	420±39	NS
More severe symptom				
Life-threatening arrhythmias	17 (36.1)	9 (33.3)	8 (40.0)	NS
Exercise-induced syncope	37 (78.7)	23 (85.2)	14 (70.0)	NS
Ventricular arrhythmia				
bVT	17 (36.2)	13 (48.1)	4 (20.0)	0.043
pVT	31 (66.0)	19 (70.4)	12 (60.0)	NS
VF	16 (34.0)	8 (29.6)	8 (40.0)	NS
Atrial arrhythmia	6 (12.8)	4 (14.8)	2 (10.0)	NS
AF	1 (2.1)	1 (3.7)	0	NS
AT	1 (2.1)	1 (3.7)	0	NS
AT	2 (4.3)	2 (7.4)	0	NS
PSVT	2 (4.3)	0	2 (10.0)	NS
Sinus bradycardia	22 (46.8)	18 (66.7)	4 (20.0)	0.014
Exercise-stress test	31 (64.8)			
Positive	30 (63.8)	19 (70.3)	11 (55.0)	NS
Negative	1 (2.1)	0	1 (5.0)	NS

Data given as mean ± SD or n (%). Mean age at onset, mean age at which patients experienced the first symptomatic arrhythmic attack or were recorded as having physical stress-induced ventricular tachycardia. Exercise stress test was considered positive for bigeminal PVCs, PVC couples, bVT, pVT, or VF. PSVT, paroxysmal supraventricular tachycardia. Other abbreviations as in Table 1.

and identified 14 mutation carriers (29.2%). Two of the family members with *RYR2* mutations experienced exercise-induced syncope (5-f, 23-f; Table 1). To confirm whether the *RYR2* mutations were inherited from the parents or not, we conducted genetic screening of the parents in 14 probands with *RYR2* mutations, and found that 8 probands were considered to carry de novo *RYR2* mutations (57.1%). In 1 patient (19-p; Table 1; arrow, Figure 3A), we identified compound heterozygous *RYR2* mutations: p.M4002I and p.K4392R. This patient was a 3-year-old boy who lost consciousness while taking a bath. His parents and siblings were all asymptomatic, and his father and sister were negative on genetic analysis. In contrast, the boy's mother (19-f1) and brother (19-f2) carried p.K4392R. Concerning p.K4392R, we identified this variant in 1 control sample from 200 normal controls. Therefore, p.M4002I was considered to be a de novo mutation and the cause of CPVT in this patient.

**CASQ2 (CPVT2)** In one of 50 probands, we identified the compound heterozygous *CASQ2* mutations p.K87X and p.W361X (Figure 3B). Both were nonsense mutations. The index patient (29-p; Table 1; Figure 3B) was a 4-year-old boy (arrow, Figure 3B) who lost consciousness at his nursery school while playing with other children and was found to have pulseless pVT in the emergency room. His parents (29-f 1 and 29-f 2) and elder brother (29-f 3) were all asymptomatic although they carried either of these 2 *CASQ2* mutations in a heterozygous state (Figure 3B).

**KCNJ2 (CPVT3)** We also identified a heterozygous missense *KCNJ2* mutation, p.G144D (Figure 2C) in one of the present probands. The proband (30-p; Table 1) was a 31-year-

old woman who had exercise-induced syncope since the age of 6. Her ECG at rest showed considerably frequent premature ventricular contractions (PVCs), which hindered the accurate measurement of U-wave. Exercise tolerance test induced bVT (Figure 1). She and her family members had neither periodic paralysis nor dysmorphic features. This patient then underwent catheter ablation therapy for PVCs and received bisoprolol fumarate (5 mg/day). The drug was not effective and was replaced with verapamil (240 mg/day). After treatment the PVCs were suppressed, and ECG showed prolonged QU intervals with prominent U-waves in the right precordial leads, suggesting phenotypic similarity with Andersen-Tawil syndrome.<sup>24</sup>

#### Proband Clinical Characteristics

Of 50 probands consecutively referred for genetic tests under the clinical diagnosis of CPVT, we excluded an asymptomatic 2-year-old proband (13-p; Table 1) and 2 with *CASQ2* and *KCNJ2* mutations. All the remaining probands were symptomatic and complained of syncope or palpitation on exercise (Table 2). Their mean age at symptom onset was 10.2±7.3 years (range, 0-39 years). Seventeen of them experienced life-threatening ventricular arrhythmias that required resuscitation, and 37 experienced repetitive exercise-induced syncope. Baseline ECG showed a normal sinus rhythm with normal QTc interval (except for 15-p in Table 1; mean QTc, 424 ms). Proband 15 had a history of repetitive syncope (15-p). We excluded this proband from the analysis of QTc interval because we suspected an additional gene mutation to cause LQTS although we failed to identify it. Regarding the dysrhythmias, bVT

Circulation Journal Vol.77, July 2013

In the beginning of 2000, genetic testing of the *RYR2* gene was performed only in some of the 105 exons of the *RYR2* gene.<sup>8,16,38</sup> Yano et al summarized more than 30 *RYR2* mutations between 2001 to 2005 and showed that most mutations were clustered in 3 main regions (3 hotspots regions): N-terminal domain, FKBP12 binding region of central domain (channel region).<sup>2,28</sup> Therefore, we first started the analysis on the 34 *RYR2* exons in the reported hotspots and then changed the protocol to examine all the exons of the *RYR2* gene. We could identify 6 additional *RYR2* mutations outside of the hotspots. The positive rate of *RYR2* mutations was increased from 41.6% to 56.0%. Similar to a previous report,<sup>38</sup> we found most of the *RYR2* mutations in the 3 main regions (70%).

The *RYR2* mutation site appeared not to be associated with phenotype differences, probably because of the relatively small number of genotyped patients. Van der Werf et al, however, extensively examined family members of *RYR2*-positive CPVT probands and found that those carrying mutations in the channel pore-forming domain had a higher prevalence of non-sustained VT than those carrying mutations in the N-terminus or central domains.<sup>28</sup>

In the present cohort, we identified a proband with compound heterozygous *CASQ2* mutations. To our knowledge, this is the second report of a compound heterozygous subject in the world.<sup>39</sup> Thus, *CASQ2* mutations can be causative of CPVT even under non-consanguineous conditions. In the first report, family members who carried either of 2 different *CASQ2* mutations also remained asymptomatic (Figure 3B).<sup>39</sup> More recently, van der Werf et al reported that the phenotype of homozygous *CASQ2* mutation carriers tends to be more malignant than those of *RYR2* mutation carriers.<sup>28</sup> By analogy to Jervell and Lange-Nielsen syndrome,<sup>31</sup> homozygous or compound heterozygous *CASQ2* mutations may cause very severe functional damage in cellular Ca-handling and thereby fatal phenotypes in probands, but not in their heterozygous relatives.

The percentage of the probands whose family members were clinically diagnosed as having CPVT was significantly larger in the *RYR2* mutation-positive group (Table 2; 33.3% vs. 5%). Van der Werf et al reported that 50% of relatives carrying an *RYR2* mutation with no CPVT phenotype at the initial cardiac evaluation developed the phenotype later during follow-up.<sup>39</sup> When *RYR2* mutations are identified in CPVT probands, the presence of *RYR2* mutation in the family members should be investigated, especially if young, even if there is an absence of clinical phenotype.

Because LQTS type 1 patients may also have exercise-related syncope,<sup>21</sup> and some have borderline or normal QTc intervals, the clinical presentation resembles that of CPVT.<sup>9</sup> Medeiros-Domingo et al found that the presence of bVT or pVT was of critical importance for differential diagnosis between CPVT and LQTS.<sup>39</sup> In the present study, exercise-induced bVT was significantly more prevalent in the *RYR2* mutation-positive patients compared to the mutation-negative patients, indicating that the exercise tolerance test would be a useful differential diagnostic tool.

Beta-blocker treatment was significantly more prevalent (P=0.027) in *RYR2* mutation-positive probands, and there was a tendency for more of them to receive combination therapy with β-blockers and verapamil or flecainide or ICD. More recently, Watanabe et al found that flecainide, a potent sodium channel blocker, prevented cardiac events in CPVT by directly inhibiting *RYR2* receptor channels.<sup>33</sup> Chan et al found that multiple pharmacological approaches targeting the Na<sup>+</sup>/Ca<sup>2+</sup> exchanger (INaCa) may be potentially useful as adjunctive

therapy to β-adrenergic blockers in suppressing CPVT-related arrhythmias.<sup>33</sup> Although preliminary, combination therapy with oral flecainide and β-blocker appeared to be most effective in preventing symptomatic arrhythmia events.

#### Conclusion

We identified 28 *RYR2* mutation carriers, 1 compound heterozygous *CASQ2* and 1 novel *KCNJ2* mutation carriers in 50 CPVT probands. This is the first report in Japan to analyze 3 different types of CPVT gene and the clinical characteristics of the genotyped CPVT patients. The percentage of the CPVT phenotype was significantly higher in *RYR2* mutation carriers than *RYR2* gene screening in CPVT patients would be indispensable to prevent unexpected cardiac sudden death of young family members.

#### References

- Swan H, Phipps K, Vitalelo M, Heikilla P, Paavonen T, Kainulainen K, et al. Arrhythmic disorder mapped to chromosome 14q24-q43 causes malignant polymorphic ventricular tachycardia in structurally normal hearts. *J Am Coll Cardiol* 1999; 34: 2055-2062.
- Laha H, Eldar M, Levy-Nissenbaum E, Bahan T, Friedman E, Khoury A, et al. Autosomal recessive catecholamine- or exercise-induced polymorphic ventricular tachycardia: Clinical features and assignment of the disease gene to chromosome 1p13-21. *Circulation* 2001; 103: 2822-2827.
- Leenhart A, Lucet V, Denjoy I, Grau F, Ngoc DD, Coumel P. Catecholaminergic polymorphic ventricular tachycardia in children: A 7-year follow-up of 21 patients. *Circulation* 1995; 91: 1512-1519.
- Bhuvan ZA, van den Berg MP, van Tintelen JP, Brink-Boelskens MT, Westdijk AC, Alders M, et al. Expanding spectrum of human *RYR2*-related disease: New electrocardiographic, structural, and genetic features. *Circulation* 2007; 116: 1569-1576.
- Sumitomo N, Sakurada H, Taniguchi K, Matsumura M, Abe O, Miyashita M, et al. Association of atrial arrhythmia and sinus node dysfunction in patients with catecholaminergic polymorphic ventricular tachycardia. *Circ* 2007; 115: 1696-1699.
- Laitinen PJ, Brown KM, Phipps K, Swan H, Devaney JM, Brambhatt B, et al. Mutations of the cardiac ryanodine receptor (*RYR2*) gene in familial polymorphic ventricular tachycardia. *Circulation* 2001; 103: 485-490.
- Postma AV, Denjoy I, Kamboj K, Alders M, Lupoglazoff JM, Viskum G, et al. Catecholaminergic polymorphic ventricular tachycardia: *RYR2* mutations, bradycardia, and follow-up of the patients. *J Mol Genet* 2005; 42: 863-870.
- Priori SG, Napolitano C, Tiso N, Memmi M, Vicari G, Bloise R, et al. Mutations in the cardiac ryanodine receptor gene (*RYR2*) underlie catecholaminergic polymorphic ventricular tachycardia. *Circulation* 2001; 103: 196-200.
- Priori SG, Napolitano C, Memmi M, Colombo B, Drago F, Gasparini M, et al. Clinical and molecular characterization of patients with catecholaminergic polymorphic ventricular tachycardia. *Circulation* 2002; 106: 69-76.
- Hasdemir C, Aydin HH, Sahin S, Wolink B. Catecholaminergic polymorphic ventricular tachycardia caused by a novel mutation in the cardiac ryanodine receptor. *Annali Karadiol* 2008; 8: E35-E36.
- Laha H, Pras E, Olender T, Avitad N, Ben-Asher E, Man O, et al. A missense mutation in a highly conserved region of *CASQ2* is associated with autonomic recessive catecholamine-induced polymorphic ventricular tachycardia in Bedouin families from Israel. *Am J Hum Genet* 2001; 69: 1378-1384.
- Vegh A, Tester D, Ackerman M, Makela J. Protein kinase A-dependent biophysical phenotype for V227F-KCNJ2 mutation in catecholaminergic polymorphic ventricular tachycardia. *Circ Arrhythm Electrophysiol* 2009; 2: 540-547.

Circulation Journal Vol.77, July 2013

Circulation Journal Vol.77, July 2013

15. Bhuiyan ZA, Hammad MA, Shamsi ET, Postma AV, Manners MM, Wilde AA, et al. A novel early onset lethal form of catecholaminergic polymorphic ventricular tachycardia maps to chromosome 7p14-p22. *J Cardiovasc Electrophysiol* 2007; 18: 1060–1066.
16. Roux-Buisson N, Clicheux M, Fourast-Lieuvin A, Fauconnier J, Brocard J, Denjoy I, et al. Absence of triadin, a protein of the calcium release complex, is responsible for cardiac arrhythmia with sudden death in human. *Hum Mol Genet* 2012; 21: 2759–2767.
17. Baucé B, Rampazzo A, Basso C, Bagatton A, Dalleno L, Tiso N, et al. Screening for ryanodine receptor type 2 mutations in families with effort-induced polymorphic ventricular arrhythmias and sudden death: Early diagnosis of asymptomatic carriers. *J Am Coll Cardiol* 2002; 40: 341–349.
18. Medeiros-Domingo A, Bhuiyan ZA, Tester DJ, Hofman N, Bikker H, van Tintelen JP, et al. The RYR2-encoded ryanodine receptor<sup>1</sup> calcium release channel in patients diagnosed previously with either catecholaminergic polymorphic ventricular tachycardia or genotype negative, exercise-induced long QT syndrome: A comprehensive open reading frame mutational analysis. *J Am Coll Cardiol* 2009; 54: 2065–2074.
19. Aizawa Y, Mitsuura W, Igarashi T, Komura S, Hanawa H, Miyajima S, et al. Human cardiac ryanodine receptor mutations in ion channel disorders in Japan. *Int J Cardiol* 2007; 116: 263–265.
20. Hayashi M, Denjoy I, Extramiana F, Mallat A, Buisson NR, Lupoglazoff JM, et al. Incidence and risk factors of arrhythmic events in catecholaminergic polymorphic ventricular tachycardia. *Circulation* 2009; 119: 2426–2434.
21. Hsieh CH, Wong YC, Chen CY, Lin TK, Lin YH, Lai LP, et al. A novel mutation (Arg169Gln) of the cardiac ryanodine receptor gene causing exercise-induced bidirectional ventricular tachycardia. *Int J Cardiol* 2006; 108: 276–278.
22. Rijnsbeek PR, Witsenburg M, Schrama E, Hess J, Kors JA. New normal limits for the paediatric electrocardiogram. *Eur Heart J* 2001; 22: 702–711.
23. Tiso N, Stephan DA, Nava A, Bagatton A, Devaney JM, Stanchi F, et al. Identification of mutations in the cardiac ryanodine receptor gene in families affected with arrhythmogenic right ventricular cardiomyopathy type 2 (ARVD2). *Hum Mol Genet* 2001; 10: 189–194.
24. Zhang L, Benson DW, Tristani-Firouzi M, Procek LJ, Tawil R, Schwartz PJ, et al. Electrocardiographic features in Andersen-Tawil syndrome patients with KCN2 mutations: Characteristic T-U-wave patterns predict the KCN2 genotype. *Circulation* 2005; 111: 2720–2726.
25. Dochi K, Watanabe H, Kawamura M, Miyamoto A, Ozawa T, Nakazawa Y, et al. Flecainide reduces ventricular arrhythmias via different actions from  $\beta$ -blockers in catecholaminergic polymorphic ventricular tachycardia. *J Arrhythmia* 2013 March 25, doi:10.1016/j.joa.2013.01.011 [Epub ahead of print].
26. Tester DJ, Arya P, Will M, Haglund CM, Farley AL, Makielski JC, et al. Genotypic heterogeneity and phenotypic mimicry among unrelated patients referred for catecholaminergic polymorphic ventricular tachycardia genetic testing. *Heart Rhythm* 2006; 3: 800–805.
27. Yano M, Yamamoto T, Ikeda Y, Matsuzaki M. Mechanisms of disease: Ryanodine receptor defects in heart failure and fatal arrhythmia. *Nat Clin Pract Cardiovasc Med* 2006; 3: 43–52.
28. Yano M. Ryanodine receptor as a new therapeutic target of heart failure and lethal arrhythmia. *Circ J* 2009; 73: 509–514.
29. van der Werf C, Noolen J, Hofman N, van Geelen N, Ehmik C, Frohn-Mulder IM, et al. Familial evaluation in catecholaminergic polymorphic ventricular tachycardia: Disease penetrance and expression in cardiac ryanodine receptor mutation-carrying relatives. *Circ Arrhythm Electrophysiol* 2012; 5: 748–756.
30. de la Fuente S, Van Langen IM, Postma AV, Bikker H, Meijer A. A case of catecholaminergic polymorphic ventricular tachycardia caused by two calstabin 2 mutations. *Pacing Clin Electrophysiol* 2008; 31: 916–919.
31. Schwartz PJ, Spazzolini C, Crotti L, Bathen J, Amlie JP, Timothy K, et al. The Jervell and Lange-Nielsen syndrome: Natural history, molecular basis, and clinical outcome. *Circulation* 2006; 113: 783–790.
32. Fukigawa M, Kawamura M, Nozaki T, Yamada Y, Miyamoto K, Okamura H, et al. Seasonal and circadian distributions of cardiac events in genotyped patients with congenital long QT syndrome. *Circ J* 2012; 76: 2112–2118.
33. Watanabe H, Chopra N, Laver D, Hwang H, Davies S, Roach D, et al. Flecainide prevents catecholaminergic polymorphic ventricular tachycardia in mice and humans. *Nat Med* 2009; 15: 380–383.
34. van der Werf C, Kannankeril PJ, Sacher F, Krahn AD, Viskin S, Leenhardt A, et al. Flecainide therapy reduces exercise-induced ventricular arrhythmias in patients with catecholaminergic polymorphic ventricular tachycardia. *J Am Coll Cardiol* 2011; 57: 2244–2254.
35. Chan YH, Wu LS, Yeh YH, Wu CT, Wang CL, Luqman N, et al. Possible targets of therapy for catecholaminergic polymorphic ventricular tachycardia: Insight from a theoretical model. *Circ J* 2011; 75: 1833–1842.

## Colorectal Carcinomas With CpG Island Methylator Phenotype 1 Frequently Contain Mutations in Chromatin Regulators

Tomomitsu Tahara,<sup>1</sup> Eiichiro Yamamoto,<sup>2,3</sup> Priyanka Madireddi,<sup>1</sup> Hiromu Suzuki,<sup>3</sup> Reo Maruyama,<sup>3</sup> Woonbok Chung,<sup>1</sup> Judith Garriga,<sup>1</sup> Jaroslav Jelinek,<sup>1</sup> Hiro-o Yamano,<sup>4</sup> Tamotsu Sugai,<sup>5</sup> Yutaka Kondo,<sup>6</sup> Minoru Toyota,<sup>3,7</sup> Jean-Pierre J. Issa,<sup>1</sup> and Marcos R. H. Estéico<sup>7,8</sup>

<sup>1</sup>Fels Institute for Cancer Research and Molecular Biology, Temple University School of Medicine, Philadelphia, Pennsylvania; <sup>2</sup>First Department of Internal Medicine and <sup>3</sup>Department of Molecular Biology, Sapporo Medical University, Sapporo, Japan; <sup>4</sup>Department of Gastroenterology, Akita Red Cross Hospital, Akita, Japan; <sup>5</sup>Department of Pathology, Iwate Medical University, Morioka, Japan; <sup>6</sup>Division of Molecular Oncology, Aichi Cancer Center Research Institute, Nagoya, Japan; <sup>7</sup>Department of Molecular Carcinogenesis and <sup>8</sup>Center for Cancer Epigenetics, The University of Texas MD Anderson Cancer Center, Houston, Texas

**BACKGROUND & AIMS:** Subgroups of colorectal carcinomas (CRCs) characterized by DNA methylation anomalies are termed CpG island methylator phenotype (CIMP1), CIMP2, or CIMP-negative. The pathogenesis of CIMP1 colorectal carcinomas, and their effects on patients' prognoses and responses to treatment, differ from those of other CRCs. We sought to identify genetic somatic alterations associated with CIMP1 CRCs. **METHODS:** We examined genomic DNA samples from 100 primary CRCs, 10 adenomas, and adjacent normal-appearing mucosae from patients undergoing surgery or colonoscopy at 3 tertiary medical centers. We performed exome sequencing of 16 colorectal tumors and their adjacent normal tissues. Extensive comparison with known somatic alterations in CRCs allowed segregation of CIMP1-exclusive alterations. The prevalence of mutations in selected genes was determined from an independent cohort. **RESULTS:** We found that genes that regulate chromatin were mutated in CIMP1 CRCs, the highest rates of mutation were observed in *CHD7* and *CHD8*, which encode members of the chromodomain helicase/adenosine triphosphatase-dependent chromatin remodeling family. Somatic mutations in these 2 genes were detected in 5 of 9 CIMP1 CRCs. A prevalence screen showed that nonsilent mutations in *CHD7* and *CHD8* occurred significantly more frequently in CIMP1 tumors (18 of 42 [43%]) than in CIMP2 (3 of 34 [9%];  $P < .01$ ) or CIMP-negative tumors (2 of 34 [6%];  $P < .001$ ). CIMP1 markers had increased binding by *CHD7*, compared with all genes. Genes altered in patients with CHARGE syndrome (congenital malformations involving the central nervous system, eye, ear, nose, and mediastinal organs) who had *CHD7* mutations were also altered in CRCs with mutations in *CHD7*. **CONCLUSIONS:** Alterations in chromatin remodeling could contribute to the development of CIMP1 CRCs. A better understanding of the biological determinants of CRCs can be achieved when these tumors are categorized according to their epigenetic status.

**Keywords:** Colon Cancer; Hypermethylation; Microsatellite Instability; Gene Silencing.

Approximately 75% of all colorectal cancers (CRCs) are sporadic and characterized by genetic lesions,

most commonly mutations of the *TP53*, *KRAS*, or *APC* gene.<sup>1,2</sup> In addition, epigenetic alterations in CRCs are also widely reported, mainly gene promoter DNA methylation. Classification of CRCs according to DNA methylation status has identified a subset of tumors with extensive epigenetic instability, characterized by concordant promoter hypermethylation.<sup>3</sup> The existence of a CpG island methylator phenotype (CIMP) and its correlation with clinicopathologic features have been confirmed extensively by use of high-throughput techniques.<sup>4,5</sup> Typical high-level CIMP (CIMP-high, CIMP1) CRCs are associated with microsatellite instability through epigenetic silencing of mismatch repair gene *MLH1*, often have *BRAF* mutation, and occur predominantly in the proximal colon, and low-level CIMP (CIMP-low, CIMP2) has been characterized by DNA methylation of a limited group of genes and mutation of *KRAS*.<sup>6</sup> Recent pathologic studies have shown that sessile serrated adenomas, mainly observed in the proximal colon, are associated with frequent *BRAF* mutation and CIMP,<sup>7</sup> suggesting that CIMP-positive CRCs arise from a different precursor than CIMP-negative tumors. Importantly, CIMP-positive CRCs are usually associated with better prognosis,<sup>8</sup> although patients with CIMP-positive CRC do not benefit from 5-fluorouracil-based adjuvant chemotherapy regimens.<sup>9</sup>

The events that lead to different clinicopathologic manifestations of CIMP1 CRCs are not well described. Although the increased frequency of DNA methylation can determine the behavior of these tumors, it is also possible that somatic mutation of a gene or a group of genes other than *BRAF* that co-occur with CIMP1 modulates the genesis and progression

<sup>1</sup>Deceased.

**Abbreviations used in this paper:** CIMP, CpG island methylator phenotype; CRC, colorectal carcinoma; SNP, single-nucleotide polymorphism; TCGA, The Cancer Genome Atlas.

© 2014 by the AGA Institute  
0016-5085/\$36.00  
http://dx.doi.org/10.1053/j.gastro.2013.10.050

of these tumors. To test this hypothesis, we used next-generation sequencing technology to analyze the exome of 16 colorectal tumors. We found that CIMP1 CRCs have frequent mutations in genes encoding proteins that function in chromatin organization, most frequently *CHD7* and *CHD8*, members of the chromodomain helicase/adenosine triphosphatase-dependent (CHD) chromatin remodeling family. These results suggest a prevalent role for aberrant chromatin remodeling in CIMP1 CRCs.

## Materials and Methods

### Preparation of Clinical Samples

We examined genomic DNA samples from 100 primary CRCs, 10 adenomas, and adjacent normal-appearing mucosae from patients undergoing surgery or colonoscopy at the Johns Hopkins Hospital, Sapporo Medical University, or Akita Red Cross Hospital. Specimens were gathered in accordance with institutional policies and all patients provided written informed consent. All DNA were obtained from frozen specimens, and none of the CRCs had been treated with chemotherapy or radiation. Tumors were selected solely on the basis of availability. Both CRCs and adenomas used in this study were characterized previously for CIMP; microsatellite instability; and *BRAF*, *KRAS*, and *TP53* mutation status.<sup>6,10</sup> For CIMP classification, DNA methylation of 7 classical markers (*p16*, *MLH1*, *MINT1*, *MINT2*, *MINT12*, *MINT31*, and *MINT313*) was evaluated by bisulfite polymerase chain reaction followed by combined bisulfite restriction analysis (COBRA) or pyrosequencing analysis. Specimens were classified as CIMP1 when *MLH1* and at least 4 of the 6 remaining markers were hypermethylated. CIMP-negative cases presented methylation of none or 1 of the markers, and CIMP2 cases were defined as those with hypermethylation of at least 2 markers but no *MLH1* hypermethylation. Adenomas were classified into CIMP groups according to the methylation profiling of their corresponding carcinoma.

### Exome Sequencing

Genomic DNA specimens from 16 colorectal tumors and their adjacent normal tissues were submitted to Orogenetics Corporation (Norcross, GA) for exome capture and sequencing. Briefly, genomic DNA was subjected to agarose gel and optical density ratio tests to confirm the purity and concentration before fragmentation. Fragmented genomic DNAs were tested for size distribution and concentration using an Agilent Bioanalyzer 2100 (Agilent Technologies, Santa Clara, CA) and a Nanodrop spectrophotometer (Thermo Fisher Scientific, Waltham, MA). Illumina libraries were made from qualified fragmented genomic DNA using Next reagents (New England Biolabs, Ipswich, MA), and the resulting libraries were subjected to exome enrichment using NimbleGen SeqCap EZ Human Exome Library v2.0 (Roche NimbleGen, Inc, Madison, WI) according to manufacturer's instructions. Libraries were tested for enrichment by quantitative polymerase chain reaction and for size distribution and concentration by an Agilent Bioanalyzer 2100. The samples were then sequenced on an Illumina HiSeq2000 (Illumina, Inc, San Diego, CA), which generated paired-end reads of 90 or 100 nucleotides. Reads from both replicates were combined in the final analysis. Data were analyzed for quality, exome coverage, and exome-wide

single-nucleotide polymorphism (SNP)/indel using the platform provided by DNAnexus (Mountain View, CA).

A sequence variation in tumor DNA was considered a potential somatic mutation if it was present in 3 or more distinct tags of at least 10 total tags. We excluded all variants with a PHRED-encoded probability score <35, those that were present in the DNA of the corresponding normal samples (excluding germline events), and those that were not in coding regions, as well as silent changes and known SNPs (except for clinically associated SNPs). The ratio of variant tag count/reference tag count was also calculated, and all variants with a ratio >0.5 were removed. DNAnexus Genome Browser was used for visual validation of all potential somatic mutations to ensure that they were present in forward and reverse strands.

### Pyrosequencing and Sanger Sequencing

Mutations in *CHD7* and *CHD8*, and selected additional mutations in 4 genes detected by exome sequencing (*ITGA10*, *CLSTN2*, *TTN*, and *KCNMA1*), were validated by pyrosequencing or Sanger sequencing. The list of primers is provided in Supplementary Table 4. Pyrosequencing was carried out on a PSQ96 system with a Pyro-Gold reagent kit (Qiagen, Valencia, CA), and the results were analyzed by PyroMark Q96 ID software version 1.0 (Qiagen). For evaluation of *CHD7* and *CHD8* genes, the coding regions from 94 additional colorectal tumors and matched normal colonic tissues were sequenced using the primers listed in Supplementary Table 11. The sequence chromatograms were visually inspected with DNA DynaScope Sequence Analysis Software (Blue Tractor Software, Llanfairfach, Wales, UK). All mutations were confirmed by independent sequencing reactions from both forward and reverse strands. Known database polymorphisms were excluded.

### Immunohistochemistry Analysis

Expression of *CHD7* (anti-*CHD7* antibody, ab31824; Abcam, Cambridge, MA) and *CHD8* (anti-*CHD8* antibody, ab84527; Abcam) was studied using the DAKO Envision system (DAKO, Carpinteria, CA), as described previously.<sup>11</sup>

### Gene Function Analysis

Functional enrichment of mutated genes was determined by gene ontology analysis using DAVID Bioinformatics Resources 6.7 (<http://david.abcc.ncifcrf.gov/>). *P* values were corrected for multiple hypothesis testing using the Benjamini method. Comparison of the spectrum of mutations in our cohort to known mutations in cancer was done using the Catalogue of Somatic Mutations in Cancer (<http://www.sanger.ac.uk/genetics/CGP/cosmic/>). Gene expression data downloaded from the Cancer Genome Atlas (TCGA) data portal (<https://tcga-data.nslb.gov/tcga/>) and published by Lalani et al were subjected to gene set enrichment analysis.<sup>12</sup>

### Statistics

The statistical significance of the differential frequency of *CHD7* and *CHD8* mutations in CIMP groups was determined using Fisher's exact test. Two-tailed *P* values were calculated using GraphPad Prism (GraphPad Software, Inc, La Jolla, CA).

## Results

### Somatic Mutations in 16 Colorectal Tumors Identified by Exome Sequencing

The clinicopathologic data for the 16 cases subjected to exome sequencing are presented in Table 1. These 16 cases consisted of 9 CIMP1 CRCs, 4 CIMP1 adenomas, 1 CIMP2 CRC, and 2 CIMP-negative CRCs. All 9 CIMP1 CRCs presented with microsatellite instability and *MLH1* epigenetic silencing, and 6 of them were known to have mutated *BRAF*. A summary of sequencing statistics for all samples can be found in Supplementary Table 1. On average, approximately 55 million purify-filtered reads were generated for each sample, and 90% of them were aligned to the genome. Samples were sequenced with a 48-fold average exon coverage (ranging from 31- to 68-fold coverage, Supplementary Table 1). Each sample was individually compared with the reference genome (hg19 build 37); single-nucleotide variants, insertions, and deletions were identified by using the DNA Nexus Mapper and nucleotide-level variation tool. Only variations in coding exons were evaluated, and germline variants were identified by comparing the tumor with normal exomes. Known variations reported in the SNP databases were filtered out (except clinically relevant SNPs), and synonymous mutations were excluded. All somatic mutations found in the 16 tumors are presented in detail in Supplementary Table 2 and are summarized in Table 2.

We found a much higher frequency of somatic mutations in CIMP1 CRCs than in other CRCs. On average, there were 425 nonsynonymous mutations per tumor, a 5-fold higher frequency than in tumors previously studied by Sjöblom et al<sup>13</sup> or Bass et al,<sup>14</sup> which were predominantly microsatellite stable tumors with wild-type *BRAF*. The frequency of mutation in the remaining cases sequenced (4 CIMP1

adenomas, 1 CIMP2 CRC, and 2 CIMP-negative CRCs) was similar to the frequency reported in other CRCs (mean 73 mutations per case) (Supplementary Table 2 and Table 2). Inversely, the nucleotide contexts of the single base substitution mutations were similar among all cases, and C to T and G to A transitions were the most frequent (Supplementary Table 3). To determine the specificity of exome sequencing, 4 randomly selected genes (*TTN*, *ITGA10*, *CLSTN2*, and *KCNMA1*) were resequenced using pyrosequencing and Sanger sequencing (Supplementary Table 4 and Supplementary Figure 1). *BRAF*, *KRAS*, and *TP53* had been previously sequenced in the tumors we used in this study, and their mutation status were included in this analysis. All 24 sequence variants detected by exome sequencing were validated by Sanger or pyrosequencing. Conversely, 12 of 13 (92%) known mutations in these cases were detected by exome sequencing. In terms of frequency of cases with mutations in genes typically associated with colon cancer, we found no mutations in *KRAS* and *SMAD4*, a case mutated for each *APC* and *PIK3CA* (6%) and 2 cases mutated for *TP53* (12%). These low frequencies were expected due to the characteristics of our group of samples, which are mostly CIMP1 (81%) or *BRAF* mutated (62%).

### Frequent Somatic Mutation of Chromatin Regulators in CIMP1 CRCs

In total, 3169 genes were somatically mutated in at least 1 CIMP1 CRC. Of these, 2615 genes were identified as mutated in other tumor types using the Catalogue of Somatic Mutations in Cancer, and 294 genes were described previously as mutated in tumors from the intestinal tract, including *BRAF*, *APC*, *TP53*, *CTNBL1*, and *PIK3CA*. To filter out genes unrelated to the CIMP phenotype in CRCs, we compared our list of mutated genes in CIMP1 CRCs with the

Table 2. Summary of Mutations in 16 Colorectal Tumors<sup>a</sup>

Cases	Total mutations	Nonsynonymous mutations	Stop codon mutations	Insertions	Deletions	SNP	MNP	5'-CpG-3'	5'-TpC-3'	Poly A tract mutations <sup>b</sup>
C709	547	526	21	40	102	392	13	123	36	67
C547	308	294	14	1	17	290	0	174	8	13
C682	94	91	3	0	1	92	1	30	8	2
C91	946	892	54	3	38	886	19	170	25	26
C658	436	411	25	3	15	409	9	475	18	13
C698	525	491	34	13	65	440	7	159	23	55
C467	418	397	21	2	15	384	7	157	21	14
C113	277	264	13	10	49	218	0	66	24	42
C391	278	265	13	0	10	268	0	93	7	9
Ad1	63	61	2	0	0	60	3	22	6	1
Ad2	80	72	8	1	1	74	4	33	5	0
Ad3	82	79	3	0	1	80	2	41	3	0
Ad4	70	65	5	0	0	68	1	32	5	0
C108	24	23	1	1	0	23	0	11	2	1
C141	122	111	11	0	0	118	4	24	4	0
C126	67	61	5	0	1	66	0	21	2	2
Total	4337	4100	236	74	315	3878	70	1631	197	245

SNP, single-nucleotide polymorphisms; MNP, multinucleotide polymorphisms.

<sup>a</sup>CIMP1 CRCs: C709, C547, C682, C91, C658, C608, C467, C113, and C391; CIMP1 adenomas: Ad1, Ad2, Ad3 and Ad4; CIMP2 CRC: C108; CIMP-negative CRCs: C141 and C126.

<sup>b</sup>Poly A tract was defined as 5 or more repeated sequences of A or T nucleotide.

lists of mutated genes in microsatellite stable, non-*BRAF*-mutated CRCs (likely CIMP-negative cases) reported in 2 exome and whole-genome analyses of colorectal tumors that together evaluated 19 cases (Supplementary Table 5).<sup>13,14</sup> As shown in Supplementary Figure 2, the overlap between our list and 1 or both of the other 2 lists was limited to 374 genes, and the majority of mutated genes were exclusive to each group.

We then performed gene ontology analysis to determine whether there was enrichment for specific functional categories among the mutated genes. This analysis showed that mutated genes in CIMP1 CRCs frequently encoded chromatin regulatory proteins ( $P = .002$  after Benjamini correction, Supplementary Table 6). Interestingly, this functional category is not represented among the genes exclusively mutated in microsatellite stable or CIMP-negative/wild-type *BRAF* cases or among the genes mutated in both tumor categories. In total, 74 of the mutated genes are included in the chromatin regulation category, and 18 of these were mutated in at least 2 cases (Figure 1 and Supplementary Table 7).

We also evaluated whether mutations in chromatin regulators were enriched in CIMP-positive CRCs in another recent exome study by the TCGA group.<sup>15</sup> We confirmed that enrichment of mutation in these 74 genes was seen more often in CIMP-high CRCs in the TCGA dataset than in CIMP-low and CIMP-negative cases (Figure 1). Among the mutated chromatin regulatory genes, lysine (K)-specific demethylase and CHD groups were particularly notable, with 6 and 5 mutated cases, respectively, in the 9 CIMP1 CRCs. Myeloid/lymphoid or mixed-lineage leukemia and SWI/SNF-related, matrix-associated, actin-dependent regulator of chromatin subfamily groups were also frequently

mutated in CIMP1 CRCs (4 cases for both groups). Although the rate of mutations in chromatin-related genes in CIMP1 adenoma cases was much lower, still 3 of 4 CIMP1 adenomas analyzed had at least 1 mutation in a chromatin-related gene.

### CHD7 and CHD8 Are Frequently Mutated in CIMP1 CRCs

Among the recurrently mutated chromatin regulatory genes, the most frequently mutated was *CHD7* (mutated in 4 cases), which encodes a member of the CHD gene family. Another member of this protein family, *CHD8*, is also present in the shortlist of candidate genes and was mutated in 3 cases. Together, these 2 genes account for mutations in >50% of the evaluated CIMP-positive CRCs (5 of 9 cases).

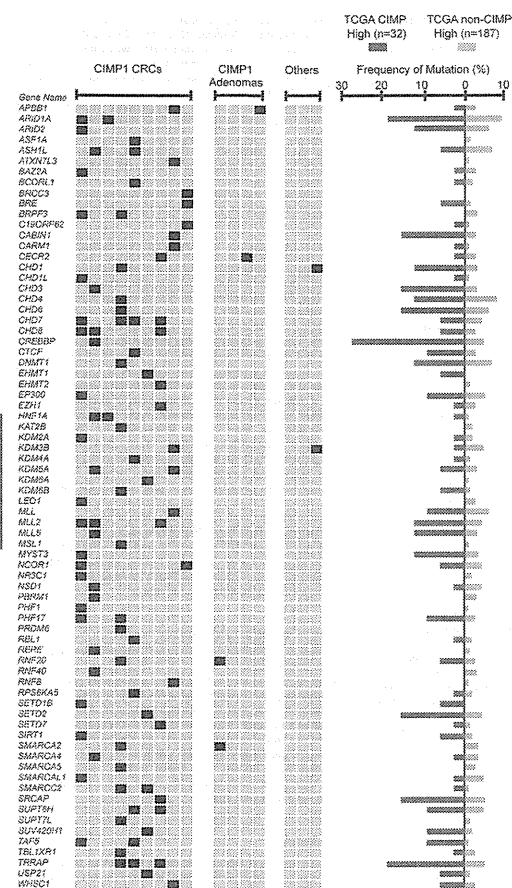
Because we compared the mutation results obtained in CIMP1 tumors with those previously published in putatively non-CIMP1 tumors, we performed a prevalence study to rule out any bias in the discovery part of this study. To confirm the association of *CHD7* and *CHD8* mutations with CIMP1, we performed Sanger sequencing of these genes in 94 additional colorectal tumors and matched normal tissues (88 CRCs and 6 adenomas; 29 were CIMP1, 33 CIMP2, and 32 CIMP-negative; Supplementary Table 8). The 2 cohorts encompassed 110 colon tumors, including 42 CIMP1, 34 CIMP2, and 34 CIMP-negative cases. Representative sequencing chromatograms are presented in Supplementary Figure 3. We found 23 cases with *CHD7* or *CHD8* nonsilent mutations. One tumor had 3 mutations, 4 had 2 mutations, and 18 had a single mutation, for a total of 29 mutations in these genes (Supplementary Table 9). Of these 29 *CHD7* and *CHD8* mutations, 24 could be compared with matched

Table 1. Clinical and Molecular Characteristics of 16 Colorectal Tumors Used in the Discovery Screen

Case	Histology	CIMP status	<i>BRAF</i> mutation <sup>a</sup>	<i>MLH1</i> methylation	MSI status	Age, y	Sex	Source of tumor DNA	Source of matched DNA
C709	Cancer	CIMP1	Wild type	Methylated	MSI	60	F	Primary tumor	Normal colon
C547	Cancer	CIMP1	Wild type	Methylated	MSI	Unknown	F	Primary tumor	Normal colon
C682	Cancer	CIMP1	Wild type	Methylated	MSI	68	F	Primary tumor	Normal colon
C91	Cancer	CIMP1	Mutated	Methylated	MSI	61	M	Primary tumor	Normal colon
C658	Cancer	CIMP1	Mutated	Methylated	MSI	83	M	Primary tumor	Normal colon
C608	Cancer	CIMP1	Mutated	Methylated	MSI	75	F	Primary tumor	Normal colon
C467	Cancer	CIMP1	Mutated	Methylated	MSI	62	M	Primary tumor	Normal colon
C113	Cancer	CIMP1	Mutated	Methylated	MSI	78	M	Primary tumor	Normal colon
C391	Cancer	CIMP1	Mutated	Methylated	MSI	63	M	Primary tumor	Normal colon
Ad1	Adenoma	CIMP1	Mutated	Unmethylated	MSI	75	M	Primary tumor	Normal colon
Ad2	Adenoma	CIMP1	Mutated	Unmethylated	MSS	83	F	Primary tumor	Normal colon
Ad3	Adenoma	CIMP1	Mutated	Unmethylated	MSS	84	F	Primary tumor	Normal colon
Ad4	Adenoma	CIMP1	Mutated	Unmethylated	MSS	77	F	Primary tumor	Normal colon
C108	Cancer	CIMP2	Wild type	Unmethylated	MSS	70	M	Primary tumor	Normal colon
C141	Cancer	CIMP-negative	Wild type	Unmethylated	MSS	60	M	Primary tumor	Normal colon
C126	Cancer	CIMP-negative	Wild type	Methylated	MSI	92	M	Primary tumor	Normal colon

MSI, microsatellite instability; MSS, microsatellite stable.

<sup>a</sup>All samples are *KRAS* wild type. C547, C391, and c141 are *TP53* mutated type; all others are *TP53* wild type.



**Figure 1.** The landscape of mutations in chromatin regulator genes identified by exome sequencing. Each row is a gene and each column is a different case. Each of the 74 chromatin regulator genes in which a mutation has been identified is listed on the left (black, mutated; light gray, wild type). The prevalence of mutations in these 74 genes in the TCGA data is shown at the right (dark gray, CIMP-high cases; light gray, non-CIMP-high cases).

genes, we mined diverse databases. *CHD7* is the most studied of the 2 genes, and mutations in *CHD7* have been reported as causative alterations in CHARGE syndrome, a complex of multiple congenital malformations involving the central nervous system, eye, ear, nose, and mediastinal organs.<sup>14</sup> We first compared distribution of *CHD7* mutations in CHARGE syndrome and CRC. From a total of 703 mutations in the *CHD7* database (www.chd7.org), we focused on 429 nonsilent pathogenic coding sequence mutations (Supplementary Figure 5, Supplementary Table 10). The most prevalent types in both CHARGE syndrome (52%) and CRC (50%) were frameshift deletions or insertions, and nonsense mutations were more frequent in CHARGE (36%) than in CRC (14%). By contrast, missense mutations were more frequent in CRC (36%) than in CHARGE (12%) (Supplementary Figure 5B). The mutations were distributed along the entire coding region, being most frequent in exon 2 in both groups, probably because it has the largest genomic size (Supplementary Figure 5A, Supplementary Table 10). Approximately 21% of the mutations were found in the regions of *CHD7* that encode for the functional domains, and all variations in CRCs observed in functional domains were located in the DEAD-like helicase superfamily (DEXDC) domain. Because the encoded region of these domains is approximately 23% of *CHD7*, the frequency of mutations within these domains is almost the same as those outside if the mutations were distributed equally (Supplementary Figure 5C).

To further assess the relationship between *CHD7* and CIMP, we analyzed publicly available data to see whether altered genes in CIMP-positive CRCs are regulated by *CHD7*.<sup>17-19</sup> We found that frequently methylated genes in CIMP-positive CRCs had significantly higher enrichment of *CHD7* occupancy in their mouse homologous genes in neural stem cells ( $P = .003$  compared with all genes; Supplementary Figure 5A) and were enriched among genes that responded to *CHD7* gene knockdown in mouse embryonic stem cells ( $P < .00001$  compared with all genes; Supplementary Figure 5B). Finally, we asked whether genes dysregulated in the CHARGE syndrome are also dysregulated in *CHD7*-mutant CRCs. For this, we downloaded level 3 gene expression data from the CRC series studied by the TCGA group.<sup>17</sup> Using gene set enrichment analysis, we asked whether genes up-regulated and down-regulated in CHARGE syndrome<sup>12</sup> are enriched among genes that distinguish *CHD7*-mutant from wild-type CRCs. We found that genes up-regulated in CHARGE syndrome are enriched among genes up-regulated in *CHD7*-mutant CRCs (false discovery rate = 0.04) and, in contrast, genes down-regulated in CHARGE syndrome are enriched among genes that are down-regulated in *CHD7*-mutant CRCs (false discovery rate = 0.07; Supplementary Figure 7). Taken together, these results indicate that the mutations in *CHD7* observed in CRCs are in many aspects functionally similar to those present in CHARGE syndrome, with effects in the regulation of dozens of genes.

Finally, we attempted to link *CHD7/8* mutations to protein levels in cancer. We identified a group of 13 samples used in the discovery and validation steps for which

paraffin-embedded tissues were available and immunohistochemistry was done for the tumors and their normal counterparts. Eleven of these were CIMP1 according to our definition, and the 2 remaining samples were CIMP-negative. Nuclear expression of these proteins was found in normal colon for all cases, and both *CHD7* and *CHD8* were variably expressed in cancers independent of their mutation status (Supplementary Figure 8). The monoallelic and single amino acid change state of the mutations can explain why changes in protein levels were not detected.

## Discussion

We found that CIMP1 CRCs have frequent mutations in genes encoding proteins that function in chromatin modification, most frequently *CHD7* and *CHD8*, members of the lysine-specific demethylases and chromatin domain helicase/adenosine triphosphate-dependent chromatin remodeling family. Molecular targets of CIMP were enriched among *CHD7*-regulated genes, and genes altered in the CHARGE syndrome with *CHD7* mutations were also altered in *CHD7*-mutant CRCs. Our data are consistent with a function of these proteins in the pathology of CIMP1 CRCs.

A confounding factor in any study that arranges tumors into CIMP groups is the criteria used for classification, as diverse strategies have been proposed and use as few as 5 to as many as 100 markers for this. Here we adopted the criterion first introduced by Toyota et al<sup>1</sup> and further refined by Shen et al,<sup>2</sup> in which 3 groups are defined based on selected markers that include hypermethylation of *MLH1* as a distinctive feature: CIMP1, CIMP2, and CIMP-negative. These groups are mostly equivalent to CIMP-high, CIMP-low, and CIMP-negative groups later defined by high throughput methylation analysis.<sup>15,16</sup> In our sequencing studies, CIMP1 CRCs presented a higher frequency of somatic mutations than CIMP1 adenomas, CIMP2 CRCs, or CIMP-negative CRCs. It is possible that the higher mutation rate in CIMP1 CRCs is linked to their mismatch repair deficiency. CIMP1 CRCs presented increased mutation in polynucleotide tracts. However, most exome mutations in CIMP1 CRCs were outside polynucleotide tracts, and one CIMP-negative, microsatellite unstable cancer we sequenced had relatively few mutations (Table 2). It is also possible that the higher mutation rate in CIMP1 CRCs is due to other factors: for example, the DNA repair gene *MGMT* was methylated in 5 of the 9 CIMP1 CRCs and in none of the other cases. The hypermutability tendency of CIMP high tumors has been described recently.<sup>15</sup>

Genes coding chromatin-related function have been reported previously as a frequent target in other tumor types,<sup>20-22</sup> but have never been clearly associated with specific subsets (eg, CIMP1 CRC). This highlights the importance of considering both genetics and epigenetics in classifying tumors for improving our understanding of the genesis and therapy for each individual tumor. Because CIMP1 CRCs differ from other CRCs in their pathologic origin, prognosis, and response to treatment,<sup>23</sup> the data suggest that the distinct genetic background reflects unique characteristics of CIMP1 cases. Unlike gliomas, the tumors

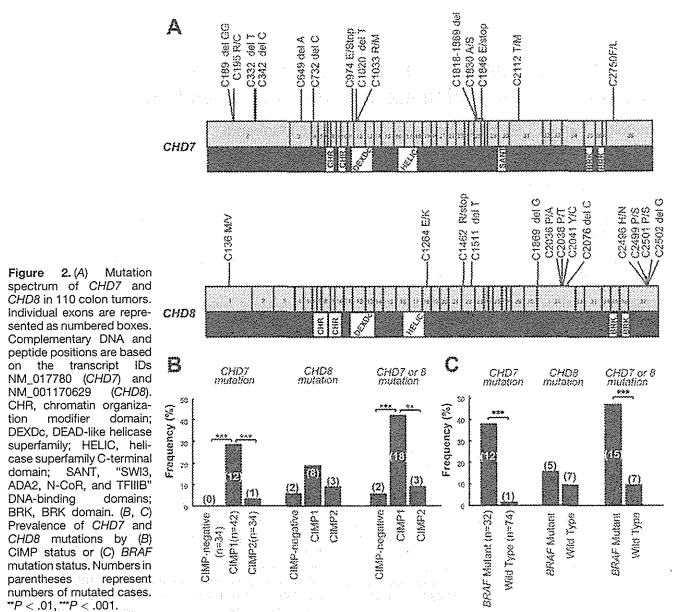


**Figure 2.** (A) Mutation spectrum of *CHD7* and *CHD8* in 110 colon tumors. Individual exons are represented as numbered boxes. Complementary DNA and peptide positions are based on the transcript IDs NM\_017780 (*CHD7*) and NM\_001170629 (*CHD8*). CHR, chromatin organization modifier domain; DEXDC, DEAD-like helicase superfamily; HELIC, helicase superfamily C-terminal domain; SANT, SWI3, ADA2, N-CoR, and TRIM7 DNA-binding domains; BRK, BRK domain. (B, C) Prevalence of *CHD7* and *CHD8* mutations by (B) CIMP status or (C) BRAF mutation status. Numbers in parentheses represent numbers of mutated cases. \* $P < .01$ , \*\*\* $P < .001$ .

normal tissues, and the remaining 5 had no matched normal tissue DNA and were compared with a reference human sequence database. The 29 nonsilent *CHD7/CHD8* mutations were distributed throughout the coding region, and 20 of them (69%) were predicted to either truncate the protein through base substitutions, resulting in a stop codon (3 mutations) or a frame deletion (12 mutations), or to damage the protein as predicted by SIFT (sorting intolerant from tolerant) analysis (5 mutations). With the exception of 2 cases with biallelic mutation of *CHD7*, all remaining variations were monoallelic. We found a significant difference in the somatic mutation rate of *CHD7* and *CHD8* genes across the molecular subtypes of colorectal tumors, with a higher incidence of mutations in the CIMP1 tumors (18 of 42 [42.9%]) than in the CIMP2 (3 of 34 [8.8%];  $P < .01$ ) or CIMP-negative tumors (2 of 34 [5.9%];  $P < .001$ ; Figure 2B).

The cases presenting *CHD7* mutations were more likely to harbor *BRAF* mutations and cases presenting *CHD7* or *CHD8* were less likely to harbor *KRAS* mutations (Figure 2C, Supplementary Figure 4A and C) or *TP53* mutation (Supplementary Figure 4B). There was also a significant association between *CHD7* and either *CHD7* or *CHD8* mutations with the presence of microsatellite instability, which is common in CIMP1 CRCs (Supplementary Figure 4D). Among adenoma cases, we found one *CHD7* mutant in a CIMP1 adenoma with microsatellite instability (Supplementary Table 9).

**Genes That Define CIMP Are *CHD7* Targets**  
The consequences of *CHD7* or *CHD8* mutation are not well established. To get insight into the functions of these

examined here had mutations in neither *IDH1* nor members of its family, indicating that different tumor types have different genetic/epigenetic interactions. Our prevalence study in a series of 94 colorectal tumors confirmed that *CHD7/CHD8* mutations occurred more frequently in CIMP1 tumors than in other CIMP groups. *CHD7* is widely expressed in many tissue types<sup>15</sup> and plays many roles in cellular differentiation<sup>24,25</sup> and chromatin regulation, including a putative role in protecting chromatin from polycomb-mediated repression.<sup>26</sup> Participation of *CHD8* in chromatin insulation has been proposed on the basis of its interaction with the well-characterized insulator protein CTCF.<sup>25,26</sup> On the basis of their function, we propose that mutations of *CHD7* and *CHD8* in CRCs result in an altered pattern of chromatin modifications and structure, which causes dysregulation of expression of dozens to hundreds of genes.

There is evidence that *CHD* genes participate in cancer. For example, *PVT1-CHD7* gene fusions have been identified in small-cell lung cancer cell lines, and a subset of gastric and colorectal cancers with microsatellite instability presented *CHD7/8* frameshift mutations in mononucleotide repeats that were associated with lower expression of *CHD8* protein.<sup>27,28</sup> In addition, mutations in *CHD5* were recently discovered in human breast cancer and neuroblastoma,<sup>29</sup> and the function of this gene as a tumor suppressor has been confirmed.<sup>30</sup> The 29 nonsilent mutations of *CHD7/8* that we identified were distributed throughout the coding region, and 69% of them (20 of 29) were predicted to truncate or damage the protein with no hot spots, a pattern concordant with that observed in tumor suppressor genes.

We also found compelling evidence that there is an overlap between genes targeted or regulated by *CHD7* and CIMP markers. Frequently methylated genes in CIMP-positive CRCs have significantly higher enrichment of *CHD7* occupancy in mouse neural stem cells and among genes regulated by *CHD7* in mouse embryonic stem cells. Evidence of a role for *CHD7* in cancer is also still lacking. In animal models, mice with homozygous *CHD7* mutations die in utero, and heterozygous mice have reduced survival at weaning.<sup>14</sup> No long-term studies could have been conducted in these models. In both CHARGE syndrome and CRC, approximately 80% of *CHD7* mutations are located outside of functional domains, suggesting that even mutations outside of key domains interfere with the gene function. Our findings and the report that a member of the *CHD* gene family has been proved to be a tumor suppressor gene<sup>31</sup> warrant evaluation of *CHD7* and *CHD8* function in colorectal tumorigenesis.

When comparing CIMP1 CRCs and adenomas, the rate of mutations in chromatin-related genes was much lower in CIMP1 adenomas. Still, 3 of the 4 CIMP1 adenomas analyzed had at least 1 mutation in a chromatin-related gene, and 1 CIMP1 adenoma in the prevalence screen presented a mutation in *CHD7* (Figure 1 and Supplementary Tables 7 and 9). In addition, the fact that *CHD7* and *CHD8* mutations were observed in subsets of microsatellite stable CRCs in our study and another study<sup>15</sup> indicates that they are not simply a consequence of defective mismatch repair. Additional functional analyses are required to better assess the

function of mutations in chromatin remodeling genes in the colorectal tumorigenesis process.

The inverse relationship between the *CHD7/8* mutations and the *TP53* inactivating mutation suggests that *CHD7/8* and *TP53* mutations drive different subsets of CRCs. Mutation of genes encoding chromatin-remodeling enzymes can result in an alternative pathway of carcinogenesis independent of *TP53* that drives cancer progression through epigenetic disturbance. The discovery of frequent chromatin regulator mutations in CIMP1 CRCs emphasizes the importance of a better understanding of pathway-specific molecular changes in subsets for targeted therapy and raises the possibility that specific epigenetic therapy targeting alterations in chromatin-remodeling proteins can be useful in treating CIMP1 CRCs.

## Supplementary Material

Note: To access the supplementary material accompanying this article, visit the online version of *Gastroenterology* at [www.gastrojournal.org](http://www.gastrojournal.org), and at <http://dx.doi.org/10.1053/j.gastro.2013.10.060>.

## References

- Rustgi AK. The genetics of hereditary colon cancer. *Genes Dev* 2007;21:2525-2538.
- Walther A, Johnstone E, Swanton C, et al. Genetic prognostic and predictive markers in colorectal cancer. *Nat Rev Cancer* 2009;9:489-499.
- Toyota M, Ohe-Toyota M, Ahuja H, et al. Distinct genetic profiles in colorectal tumors with or without the CpG island methylator phenotype. *Proc Natl Acad Sci U S A* 2000;97:710-715.
- Estacio MR, Yan PS, Ibrahim AE, et al. High-throughput methylation profiling by MCA coupled to CpG island microarray. *Genome Res* 2007;17:1529-1536.
- Weisenberger DJ, Siegmund KD, Campan M, et al. CpG island methylator phenotype underlies sporadic microsatellite instability and is tightly associated with BRAF mutation in colorectal cancer. *Nat Genet* 2006;38:787-793.
- Shen L, Toyota M, Kondo Y, et al. Integrated genetic and epigenetic analysis identifies three distinct subclasses of CpG island methylator phenotype colorectal cancer. *Proc Natl Acad Sci U S A* 2007;104:18654-18659.
- Leggett B, Whitehall V. Role of the serrated pathway in colorectal cancer pathogenesis. *Gastroenterology* 2010;138:2088-2100.
- Ogino S, Nosho K, Kirkner GJ, et al. CpG island methylator phenotype, microsatellite instability, BRAF mutation and clinical outcome in colon cancer. *Gut* 2009;58:90-96.
- Jovar R, Nguyen TP, Perez-Carbonell L, et al. 5-Fluorouracil adjuvant chemotherapy does not increase survival in patients with CpG island methylator phenotype colorectal cancer. *Gastroenterology* 2011;140:1174-1181.
- Kimura T, Yamamoto E, Yamano HG, et al. A novel pit pattern identifies the precursor of colorectal cancer derived from sessile serrated adenoma. *Am J Gastroenterol* 2012;107:460-469.

11. Sugai T, Habano W, Uesugi N, et al. Three independent genetic profiles based on mucin expression in early differentiated-type gastric cancers—a new concept of genetic carcinogenesis of early differentiated-type adenocarcinomas. *Mod Pathol* 2004;17:1223–1234.

12. Lalani SR, Safiullah AM, Fernbach SD, et al. Spectrum of CHD7 mutations in 110 individuals with CHARGE syndrome and genotype-phenotype correlation. *Am J Hum Genet* 2006;78:303–314.

13. Sjöblom T, Jones S, Wood LD, Parsons DW, et al. The consensus coding sequences of human breast and colorectal cancers. *Science* 2006;314:268–274.

14. Bass AJ, Lawrence MS, Bracci LE, et al. Genomic sequencing of colorectal adenocarcinomas identifies a recurrent VTI1A-TCF7L2 fusion. *Nat Genet* 2011;43:964–968.

15. The Cancer Genome Atlas Research Network. Comprehensive molecular characterization of human colon and rectal cancer. *Nature* 2012;487:330–337.

16. Janssen N, Bergman JE, Swertz MA, et al. Mutation update on the CHD7 gene involved in CHARGE syndrome. *Hum Mutat* 2012;33:1149–1160.

17. Ergülen E, Akinci U, Bryra JC, et al. Sox2 cooperates with CHD7 to repress genes that are mutated in human syndromes. *Nat Genet* 2011;43:607–611.

18. Hinooue T, Weisenberger DJ, Lange CP, et al. Genome-scale analysis of aberrant DNA methylation in colorectal cancer. *Genome Res* 2012;22:271–282.

19. Schetz MP, Handoko L, Akhtar-Zaidi B, et al. CHD7 targets active gene enhancer elements to modulate ES cell-specific gene expression. *PLoS Genet* 2010;6:e1001023.

20. Jones S, Wang TL, Shih LE, et al. Frequent mutations of chromatin remodeling gene ARID1A in ovarian clear cell carcinoma. *Science* 2010;330:228–231.

21. van Haafren G, Dalgliesh GL, Davies H, et al. Somatic mutations of the histone H3K27 demethylase gene UTX in human cancer. *Nat Genet* 2009;41:521–523.

22. Wilson BG, Roberts CW. SWI/SNF nucleosome remodelers and cancer. *Nat Rev Cancer* 2011;11:481–492.

23. Bajpai R, Chen DA, Rada-Iglesias A, et al. CHD7 cooperates with PBAF to control multipotent neural crest formation. *Nature* 2010;463:958–962.

24. Srinivasan S, Dorigi KM, Tamkun JW. *Drosophila* Kismet regulates histone H3 lysine 27 methylation and early elongation by RNA polymerase II. *PLoS Genet* 2006;4:e1000217.

25. Huang S, Li X, Yusufzai TM, et al. USP1 recruits histone modification complexes and is critical for maintenance of a epigenetic barrier. *Mol Cell Biol* 2007;27:7951–7955.

26. Ishihara K, Oshimura M, Hatako M. CTCF-dependent chromatin insulator is linked to epigenetic remodeling. *Mol Cell* 2006;23:733–742.

27. Kim MS, Chung NG, Kang MR, et al. Genetic and expression alterations of CHD genes in gastric and colorectal cancers. *Histopathology* 2011;58:660–668.

28. Plesance ED, Stephens PJ, O'Meara S, et al. A small-cell lung cancer genome with complex signatures of tobacco exposure. *Nature* 2010;463:194–199.

29. Bagchi A, Mills AA. The quest for the 1p36 tumor suppressor. *Cancer Res* 2009;69:2551–2556.

30. Bagchi A, Papazoglu C, Wu Y, et al. CHD6 is a tumor suppressor at human 1p36. *Cell* 2007;128:459–475.

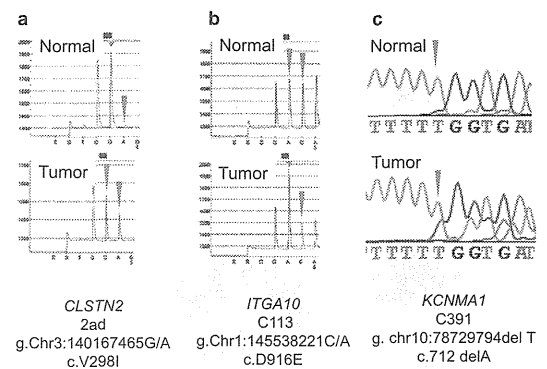
Author names in bold designate shared co-first authorship.

**Reprint requests**  
Address requests for reprints to: Marcos R. H. Estêvão, PhD, Department of Molecular Carcinogenesis, The University of Texas MD Anderson Cancer Center, 1515 Holcombe Boulevard, Houston, Texas 77030. e-mail: mesteavo@mdanderson.org; fax: (512) 237-3439.

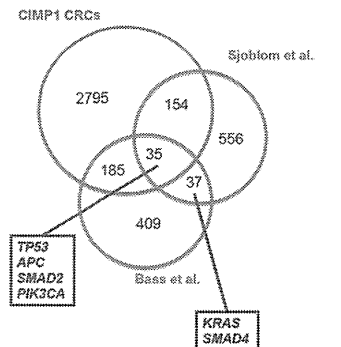
**Acknowledgments**  
The authors thank Kathryn L. Hale for proofreading the manuscript.

**Conflicts of interest**  
The authors disclose no conflicts.

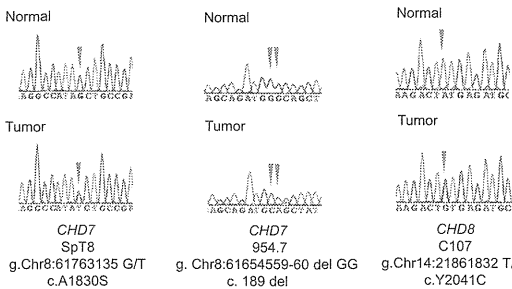
**Funding**  
This work was supported by the G.S. Hogan Gastrointestinal Research Fund of The University of Texas MD Anderson Cancer Center (to M.R.H.E.) and by National Institutes of Health grants CA158112, CA096806, and CA100632 to J.-P.J.I. J.-P.J.I. is an American Cancer Society Clinical Research professor supported by a generous gift from the F.M. Kirby Foundation.



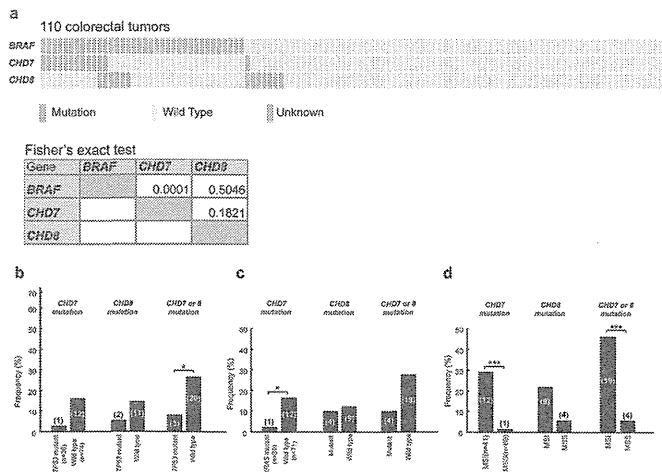
Supplementary Figure 1. Representative pyrograms (A and B) and sequencing chromatograms (C) for 3 of 4 randomly selected genes mutated in the discovery set.



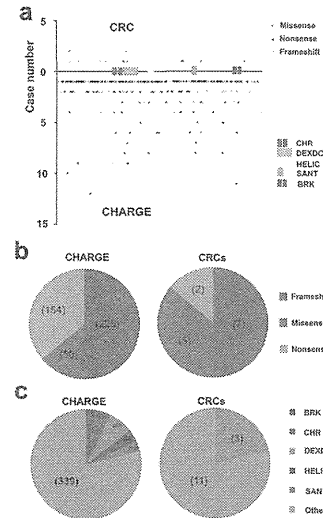
Supplementary Figure 2. Venn diagram representing the number of genes mutated in CIMP1 CRCs, microsatellite stable/wild-type BRAF CRCs, and non-CIMP-high/unmethylated/wild-type BRAF CRCs in our study and 2 other studies. Nearly 3000 genes were mutated exclusively in the CIMP1 CRCs.



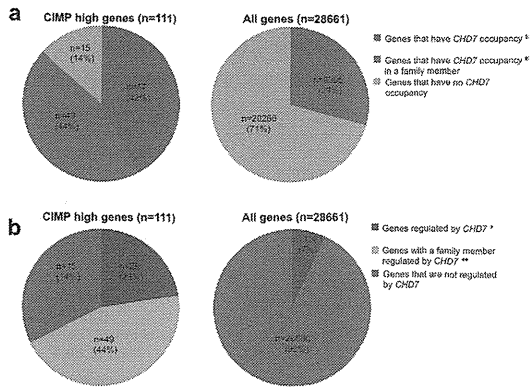
Supplementary Figure 3. Representative sequencing chromatograms of CHD7 and CHD8 genes in validation samples.



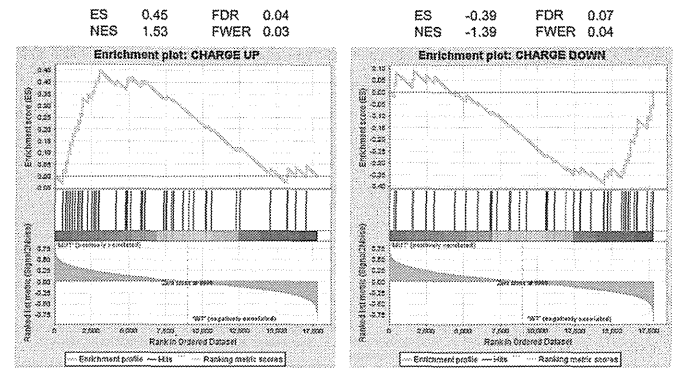
Supplementary Figure 4. Presence of mutations in BRAF, CHD7, and CHD8 in 110 colorectal tumors (A). P values of Fisher's exact test are shown. BRAF and CHD7 show a strong tendency of co-occurrence in the test samples. Prevalence of CHD7 and CHD8 mutations by different TP53 (B) and KRAS mutations (C) and microsatellite stability status (D). Numbers in parentheses represent the number of mutated cases. MSI, microsatellite instability; MSS, microsatellite stability. \*P < .05; \*\*\*P < .001.



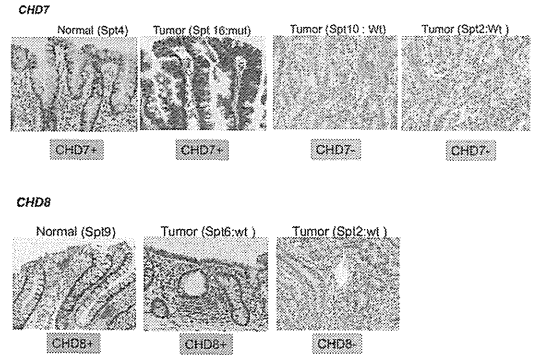
Supplementary Figure 5. Comparison of CHD7 mutation spectra in CHARGE syndrome and CRC. A total of 429 nonsilent pathogenic coding sequence mutations in CHARGE syndrome (from the database [www.chs7.org](http://www.chs7.org)) were used for this analysis. (A) Overview of nonsilent pathogenic coding sequence mutations in CHARGE syndrome (upper) and CRC (lower). Each plot represents a single mutation, and the x-axis represents the number of reported cases. (B, C) CHD7 change types (B) and distribution across domains (C) in CHARGE syndrome (left) and CRC (right). Numbers in parentheses represent number of mutations. BRK, BRK domain; CHR, chromatin organization modifier domain; DEXDC, DEAD-like helicase superfamily; HELIC, helicase superfamily C-terminal domain; SANT, "SWI3, ADA2, N-CoR and TFIIB" DNA-binding domains.



**Supplementary Figure 6.** Enrichment of *CHD7* occupancy in frequently methylated genes in CIMP-positive CRCs (A) and greater influence of *CHD7* gene knockdown on gene expression change (B). The genes used for comparisons were hypermethylated with a  $\beta$ -value difference >0.20 and showed >2-fold decrease in their gene expression levels in CIMP-high tumors, as reported by Hinoue et al<sup>13</sup> (n = 111). Genes bound by Chd7 in mouse neural stem cells (Engelen et al<sup>14</sup>) and altered expression after knockdown of *CHD7* in mouse ES cells (Schnetz et al<sup>15</sup>) were considered to be regulated by *CHD7*. <sup>‡</sup>CIMP genes,  $P = .003$ ; <sup>‡\*</sup>CIMP genes and their family members,  $P < .00001$  compared with all genes. <sup>‡</sup>CIMP genes,  $P < .00001$ ; <sup>‡\*</sup>CIMP genes and their family members,  $P < .00001$  compared with all genes.



**Supplementary Figure 7.** GSEA on TCGA CRC dataset (*CHD7*-mut versus *CHD7*-wt). **Supplementary Figure 7.** Enrichment of genes up-regulated and down-regulated in CHARGE syndrome among classifiers of *CHD7*-mutant CRCs. GSEA, gene set enrichment analysis; MUT, mutant; WT, wild type.



**Supplementary Figure 8.** Immunohistochemical (IHC) analysis of *CHD7* and *CHD8* in normal colon and colorectal tumors with and without *CHD7/8* mutations.



厚生労働科学研究費補助金 地域医療基盤開発推進研究事業

遠隔医療を実施する拠点病院のあり方に関する研究

平成 24-25 年度 総合研究報告書

発行日 平成 26 年 3 月

発行者 岩手医科大学 小川 彰

〒020-8505 岩手県盛岡市内丸 19-1

TEL019-651-5111 (代)

発行所 橋本印刷



